JACS
JOURNAL OF THE AMERICAN CHEMICAL SOCIETY
Article
pubs.acs.org/JACS

Conformations and Fluorescence of Encapsulated Stilbene

Demeter Tzeli,[†] Giannoula Theodorakopoulos,[†] Ioannis D. Petsalakis,*[,†] Dariush Ajami,[‡] and Julius Rebek, Jr.[‡]

[†]Theoretical and Physical Chemistry Institute, National Hellenic Research Foundation, 48 Vassileos Constantinou, Athens 116 35, Greece

[‡]The Skaggs Institute for Chemical Biology & Department of Chemistry, The Scripps Research Institute, 10550 North Torrey Pines Road, La Jolla, California 92037, United States

Supporting Information

ABSTRACT: Absorption and emission spectra of free and encapsulated stilbene in two different capsules were calculated using the DFT and the TDDFT methodology at the B3LYP, CAM-B3LYP, M06-2X, PBE0, and ωB97X-D/6-31G(d,p) levels of theory. The present work is directed toward the theoretical interpretation of recent experimental results on control of stilbene conformation and fluorescence in capsules [Ams, M. R.; et al. *Beilstein J. Org. Chem.* **2009**, *5*, 79]. The results of the calculations are in agreement with experiment and show that fluorescence of *trans*-stilbene persists in the large cage while it is quenched in the small one. It is found that the geometry of *trans*-stilbene in the ground as well as in the first excited singlet state is unaffected by encapsulation in the large cage, and consequently the absorption and emission spectra are similarly unaffected. In the small cage, the ground state of encapsulated *trans*-stilbene is distorted, with the two phenyl groups twisted, while the geometry of the excited state, after relaxation, lies at the conical intersection with the ground state. Consequently, there is no emission similar to that of free *trans*-stilbene, and the state decays nonradiatively to the ground state.

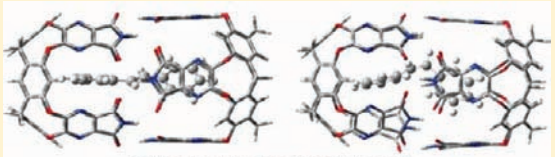
Stilbene ground and excited states

1. INTRODUCTION

Over the past 65 years, photoisomerization of stilbene (1,2-diphenylethylene) and its derivatives has been studied because of their important role in many areas of chemistry,[1−6] in photophysics,[1,6,7] and in material science.[8] Moreover, as shown by the number of recent publications, there is continuing interest in this topic.[9−28] Stilbene has been regarded as a model system for photochemical dynamics with regard to trans−cis isomerization (see Scheme 1 and Figure 1), and it is generally accepted that upon photoexcitation from S_0 to S_2, stilbene rapidly decays to S_1, where both the trans and the cis isomers decay to S_0 via a conical intersection[1,6,13,24] (cf. Scheme 1).

Scheme 1. Schematic Representation of the Isomerization

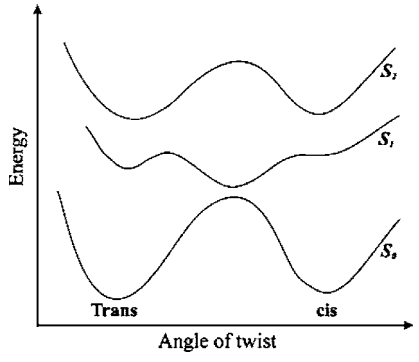

trans-Stilbene in the ground and first two singlet excited states has been investigated the most thoroughly. The planarity of free *trans*-stilbene is an issue that has been a source of some controversy both theoretically (via ab initio methods) and experimentally, because the two phenyl groups can rotate with a very low energy cost. The minimum energy structures, vibrational motions, and dynamics mainly of S_0 and the two lowest singlet excited states S_1 and S_2, and in some cases of a few additional singlet and triplet excited states, have been investigated both experimentally via crystallographic and a variety of spectroscopic techniques[9−16] and theoretically.[14−28] A great variety of theoretical methods have been employed for calculations on stilbene including semiempirical,[15,17] CASSCF,[18−21] CASPT2,[18] MP2,[22,23] CIS,[16] MMVB,[25] CCSD(T),[23] DFT and TDDFT (B3LYP),[16a,19,21,26] TDDFT(PBE0),[14,24] spin-flip DFT,[27] and semiclassical electron-radiation-ion dynamics.[28]

It is well known that *trans*-stilbene gives weak fluorescence in solution and inside loosely fitting capsules,[29] while intense blue fluorescence has been observed from stilbene in a complex with an antibody.[30] Fluorescence of *trans*-stilbene inside a tight-fitting capsule is greatly reduced, to only 2% of the fluorescence in bulk solution,[29] which is an unexpected result in view of the antibody studies, and it has been attributed to a distortion of the ground state conformation in the tight-fitting capsule. The reversible encapsulation of molecules provides a means of temporarily isolating molecules in the solution phase but removed from bulk solvent.[31,32] It can lead to the control of their geometric photochemical isomerization and photoreactions,[33−35] or

Received: November 29, 2011
Published: January 30, 2012

   dx.doi.org/10.1021/ja211164b | *J. Am. Chem. Soc.* 2012, 134, 4346−4354

Figure 1. Optimized structures for *trans*-stilbene, *cis*-stilbene, and the transition state for isomerization of the stilbene.

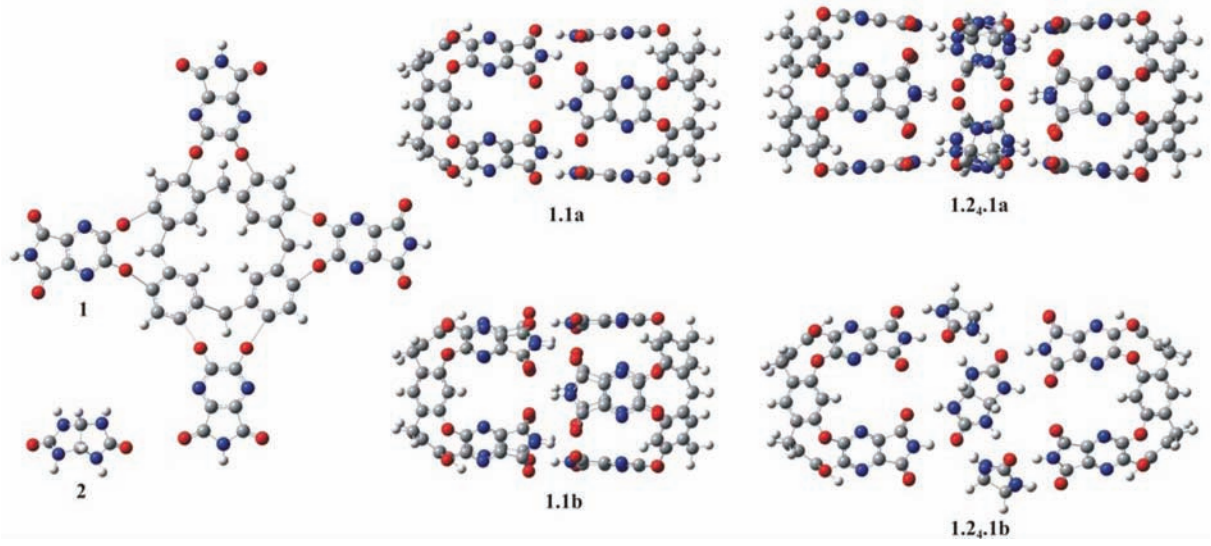

Figure 2. Structures of the cavitand **1** and glycoluril **2** components and structures of the cages **1.1** and **1.2$_4$.1**. H atoms = white spheres, C = gray spheres, O = red spheres, and N = blue spheres.

through photoisomerization the reversible encapsulation can be controlled, i.e., switch between different capsule assemblies.[36] The encapsulation of *trans*-stilbene involved self-assembled complexes **1.1** and **1.2$_4$.1**, shown in Figure 2, formed by two cavitands **1** and in addition four glycoluril molecules **2**,[37] respectively.

In the present work, the encapsulation of *trans*-stilbene in the self-assembled complexes **1.1** and **1.2$_4$.1** is studied theoretically using density functional theory (DFT) and the time-dependent DFT (TD-DFT) methodology. For the **1.2$_4$.1** capsule we calculated two isomers, **a** and **b** (see Figure 2). The objective of the present study was to calculate the fluorescence spectra of *trans*-stilbene, free as well as encapsulated in the **1.1** and **1.2$_4$.1** capsules, and thus to determine how the possible distortion of the ground-state geometry in the **1.1** capsule leads to the observed fluorescence quenching.[30]

2. COMPUTATIONAL DETAILS

The encapsulation and the absorption and emission spectra of *trans*-stilbene in **1.1** and **1.2$_4$.1** capsules were studied as mentioned above using the DFT and the TDDFT methodology. The DFT and TDDFT calculations were carried out using different functionals for comparison, namely B3LYP,[38] CAM-B3LYP,[39] M06-2X,[40] PBE0,[41] and ωB97X-D,[42] in conjunction with the 6-31G(d,p)[43] basis sets. B3LYP is a widely used functional and generally works well for main-group chemistry. The CAM-B3LYP functional has been developed to correct for the long-range behavior.[39] M06-2X is a functional recommended for applications involving main-group elements, kinetics, noncovalent interactions, and electronic excitation energies to valence and Rydberg states.[40] The PBE0 (or PBE1PBE) functional is obtained combining the PBE generalized gradient functional with a predefined amount of exact exchange. It uses 25% exchange and 75% correlation weighting. The way in which the functional is derived and the lack of empirical parameters fitted to specific properties make the PBE0 model a widely applicable method.[41] The ωB97X-D functional includes 100% long-range exact exchange, a small fraction of short-range exact exchange, a modified B97 exchange density functional for short-range interaction, and empirical dispersion corrections.[42] In conjunction with the above functionals, the 6-31G(d,p) basis set is employed, which is considered to be a good compromise for adequate accuracy since the number of atoms (up to 300 atoms) in the encapsulated complexes is too big for larger basis sets. Moreover, previous study on encapsulation of molecules[32] in cages shows that the 6-31G(d,p) basis set in conjunction with the M06-2X functional presents good results.

The computational strategy followed involved (i) geometry optimization of free *trans*-stilbene, the encapsulated forms (in **1.1** and **1.2$_4$.1** of Figure 2), and the free capsules and (ii) TDDFT determination of the absorption and emission spectra of free and encapsulated *trans*-stilbene. In addition, geometry optimization has been carried out, as well as the absorption and emission spectra of free and encapsulated (in **1.1**) *cis*-stilbene. In greater detail,

(i) DFT geometry optimization calculations were performed on the ground electronic state of free *trans*-stilbene, *cis*-stilbene, and the transition state (cf. Figure 1) using the different functionals (see above). Geometry optimization of the encapsulation complexes was carried out using the ONIOM[44] method, where the systems were defined as two regions (layers) with the high layer, which is the stilbene, calculated at the B3LYP, CAM-B3LYP, M06-2X, PBE0, and ωB97X-D/6-31G(d,p) levels and the low layer, which is the capsule, calculated at the PM6 level of theory. Finally, DFT geometry optimization calculations for the full encapsulation complexes (without the OMIOM procedure) were carried out at the B3LYP, CAM-B3LYP, M06-2X, and PBE0/6-31G(d,p) levels of theory and single point calculations at the ωB97X-D/6-31G(d,p)//M06-2X/6-31G(d,p) level of theory. For all determined structures, basis set superposition error (BSSE) corrections have been taken into account using the counterpoise procedure[45] since such corrections are important for weak and medium-size interactions,[46] which is the case for the structures calculated here.

dx.doi.org/10.1021/ja211164b | J. Am. Chem. Soc. 2012, 134, 4346−4354

(ii) Straightforward TDDFT calculations yield the absorption spectrum of free stilbene, and with some more computational effort, involving geometry optimization of the first singlet excited state, the fluorescence spectrum is obtained. However, for the encapsulation complexes, many excited states of the cage lie below the state relevant to stilbene absorption, and consequently it was not possible to determine it directly by TDDFT on the full complex. For example, calculation of the absorption spectra of 60 singlet-spin excited electronic states of the encapsulated complex **1.1**_*trans*-stilbene did not yield any excited states of stilbene. This calculation was carried out at the B3LYP/4-31G level of theory, because there were technical difficulties with the use of the 6-31G(d,p) basis set. In view of the fact that even 60 roots are not sufficient and the calculation of a larger number of roots even at the B3LYP/4-31G level of theory presented technical difficulties, the TDDFT calculations on the full complex were not pursued any further. The absorption spectrum of encapsulated *trans*-stilbene was obtained by carrying out TDDFT calculations on free *trans*-stilbene but at its optimum geometry in the encapsulated complexes. Second, the absorption spectra of the encapsulated complexes were determined using the ONIOM methodology as described above, where the DFT and TDDFT calculations involve only the electronic states of *trans*-stilbene and not the capsule. It must be noted that the ONIOM methodology is the only option for the determination of the fluorescence spectra of the encapsulation complexes, since optimization of the geometry of the excited state within the cage is required. For the above calculations of the absorption and emission spectra of free and encapsulated stilbene, twenty to thirty singlet spin excited electronic states have been calculated by TDDFT[47] calculations.

All calculations were performed using the Gaussian 09 program package.[48] The coordinates of all the optimum structures are included in the Supporting Information (SI).

3. RESULTS AND DISCUSSION

3.1. Geometry. Geometry optimization on encapsulated complex **1.1_t**, of *trans*-stilbene (**t**) in the small cage (**1.1**), was carried out employing all five functionals (see above). It should be noted that only in the case of the B3LYP functional, two nearly energetically equal isomers of the **1.1** cage, i.e. **1.1a** and **1.1b**, and similarly two nearly energetically equal isomers of the **1.1_t** species, i.e. **1.1a_t** and **1.1b_t**, were calculated (see Figures 2 and 3 and Figure 1S of the SI). In both cases, the difference in geometry between the **a** and **b** isomers is that the cage is slightly twisted in **b** (Figure 2), with a difference in energy under 0.03 eV. With the remaining functionals, PBE0, M06-2X, and ωB97X-D, in case of the free cage (**1.1**), the geometry optimization results in the **1.1a** minimum only, while for the encapsulated complex (**1.1_t**), only the **b** isomer is found as a stable structure; i.e., **1.1b** and **1.1a_t** are not found as stable structures in the geometry optimizations. Finally, calculations on the encapsulation of *cis*-stilbene resulted in the **1.1a_c** complex (cf. Figure 3). It might be noted that even

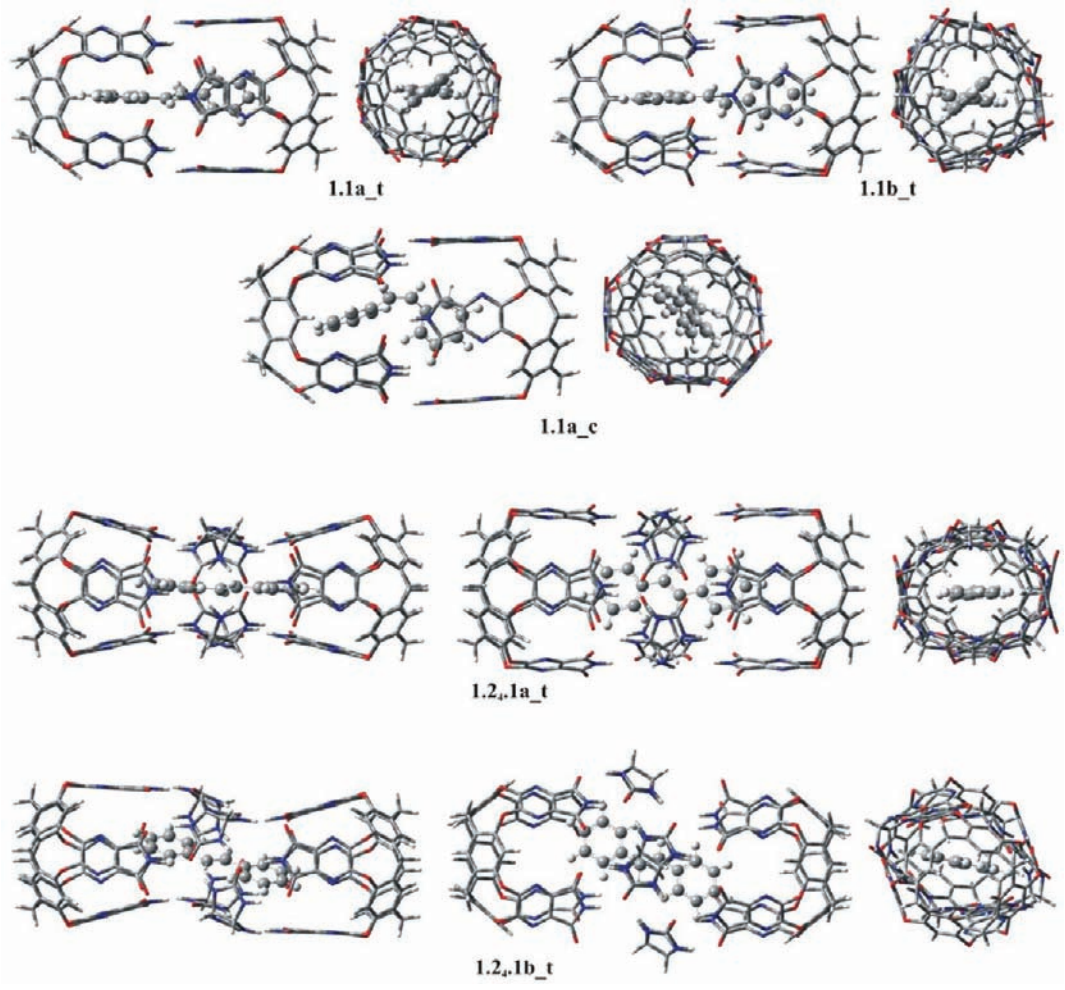

Figure 3. Optimized structures of encapsulated *trans*-stilbene (**t**) and *cis*-stilbene (**c**) in the capsules **1.1** and **1.2$_4$.1** viewed from two or three different angles, i.e, along the central axis of the capsule and end-on view. H atoms = white spheres, C = gray spheres, O = red spheres, and N = blue spheres. The atoms of the capsule are designed with stick bonds for clarity.

dx.doi.org/10.1021/ja211164b | *J. Am. Chem. Soc.* 2012, 134, 4346−4354

Table 1. Bond Lengths (in Å), Bond Angles, and Dihedral Angles (in Deg) of *trans*-Stilbene, *cis*-Stilbene, and the Encapsulation Complexes 1.1_t, 1.1_c, and 1.2$_4$.1_t in the Ground (S_0) and First Excited (S_1) States at Various Levels of Theory

	trans-stilbene (S_0)			*trans*-stilbene (S_1)			**1.1a_t** (S_0)		**1.1b_t** (S_0)	
	B3LYP	PBE0	M06-2X	B3LYP	PBE0	M06-2X	B3LYP	B3LYP	PBE0	M06-2X
C_1-C_2	1.348	1.345	1.341	1.416	1.413	1.418	1.348	1.348	1.346	1.344
C_1-C_3	1.466	1.461	1.469	1.415	1.410	1.407	1.467	1.467	1.464	1.472
C_2-C_4	1.466	1.461	1.469	1.415	1.410	1.407	1.467	1.467	1.464	1.473
C_1-H_1	1.089	1.089	1.089	1.087	1.087	1.086	1.089	1.089	1.090	1.092
C_2-H_2	1.089	1.089	1.089	1.087	1.087	1.086	1.089	1.089	1.090	1.092
$C_4C_2C_1$	127.2	127.0	126.6	125.6	125.3	125.0	126.0	126.2	126.2	124.8
$C_2C_1C_3$	127.2	127.0	126.6	125.6	125.3	125.0	126.0	126.1	125.6	125.2
$C_4C_2H_2$	114.1	114.2	114.4	116.2	116.3	116.5	115.1	115.0	115.0	115.7
$C_3C_1H_1$	114.1	114.2	114.4	116.2	116.3	116.5	115.1	115.0	115.2	115.7
$C_4C_2C_1C_3$[a]	180.0	180.0	180.0	179.9	179.9	179.8	176.9	176.9	176.8	172.3
$d_{ph\text{-}ph}$[b]	0.4	0.5	0.4	0.2	0.2	0.3	43.5	41.9	41.3	49.3
	1.2$_4$.1a_t (S_0)			**1.2$_4$.1b_t** (S_0)			*cis*-stilbene (S_0)			**1.1a_c** (S_0)
	B3LYP	PBE0	M06-2X	B3LYP	PBE0	M06-2X	B3LYP	PBE0	M06-2X	B3LYP
C_1-C_2	1.349	1.346	1.342	1.349	1.346	1.342	1.349	1.346	1.341	1.350
C_1-C_3	1.467	1.462	1.471	1.467	1.463	1.470	1.475	1.470	1.478	1.473
C_2-C_4	1.467	1.463	1.472	1.467	1.463	1.470	1.475	1.470	1.478	1.471
C_1-H_1	1.088	1.089	1.091	1.087	1.088	1.089	1.090	1.090	1.089	1.086
C_2-H_2	1.088	1.089	1.093	1.087	1.088	1.089	1.090	1.090	1.089	1.089
$C_4C_2C_1$	127.0	126.2	124.9	127.0	126.8	126.0	131.2	130.3	128.3	131.7
$C_2C_1C_3$	127.0	127.2	127.0	127.0	126.8	126.0	131.2	130.3	128.3	132.7
$C_4C_2H_2$	114.3	114.7	115.3	114.1	114.2	114.3	113.4	113.9	114.7	113.5
$C_3C_1H_1$	114.3	114.2	113.7	114.0	114.2	114.3	113.4	113.9	114.7	112.9
$C_4C_2C_1C_3$[a]	179.7	179.6	179.0	180.0	180.0	180.0	7.1	7.0	6.4	10.7
$d_{ph\text{-}ph}$[b]	18.1	16.5	3.4	1.4	0.0	0.0	128.1	127.4	125.8	126.4
	1.1b_t (S_1)			**1.2$_4$.1a_t** (S_1)			**1.2$_4$.1b_t** (S_1)			
	B3LYP[c]	PBE0[c]	M06-2X[c]	B3LYP[c]	PBE0[c]	M06-2X[c]	B3LYP[c]	PBE0[c]	M06-2X[c]	
C_1-C_2	1.443	1.435	1.436	1.417	1.414	1.419	1.417	1.414	1.419	
C_1-C_3	1.421	1.419	1.426	1.414	1.409	1.406	1.415	1.410	1.407	
C_2-C_4	1.418	1.415	1.423	1.416	1.411	1.407	1.415	1.410	1.407	
C_1-H_1	1.100	1.101	1.098	1.088	1.089	1.088	1.088	1.088	1.087	
C_2-H_2	1.092	1.095	1.092	1.088	1.089	1.088	1.088	1.088	1.087	
$C_4C_2C_1$	126.1	125.6	125.4	125.1	124.8	124.4	125.5	125.2	124.8	
$C_2C_1C_3$	127.6	126.9	127.1	125.7	125.5	125.0	125.5	125.2	124.8	
$C_4C_2H_2$	115.4	115.7	115.2	116.6	116.8	117.0	116.1	116.2	116.5	
$C_3C_1H_1$	113.5	114.0	113.5	115.8	115.9	116.2	116.1	116.2	116.5	
$C_4C_2C_1C_3$[a]	93.8	96.0	94.0	179.3	179.6	179.0	180.0	179.8	180.0	
$d_{ph\text{-}ph}$[b]	69.7	69.0	69.0	5.8	6.1	7.2	0.0	0.3	0.0	

[a]Dihedral angle between the (C_4,C_2,C_1) and (C_2,C_1,C_3) planes. [b]Dihedral angle between the two phenyl groups, i.e, between the ($C_7C_4C_8$) and ($C_5C_3C_6$) planes. [c]ONIOM(A/6-31G(d,p):PM6), A = B3LYP, PBE0, and M06-2X.

though an exhaustive search of the potential energy surface has not been made, trial optimization of other possible structures for the **1.1** and **1.1_t** species resulted only in the above minimum structures (cf. Figures 2 and 3).

Two isomers for the **1.2$_4$.1** cage, i.e. **1.2$_4$.1a** and **1.2$_4$.1b** (see Figure 2), which consists of two cavitands **1** and four glycoluril molecules **2**, were obtained by all functionals. These two isomers differ in the relative position of the glycoluril molecules. In the **1.2$_4$.1a** isomer each glycoluril molecule forms hydrogen bonds with both cavitands and with its adjacent glycoluril molecules. In contrast, in the **1.2$_4$.1b** isomer, two glycoluril molecules form hydrogen bonds with both cavitands and with their adjacent glycoluril molecules; the other two glycoluril molecules form hydrogen bonds with only one cavitand and with their two adjacent glycoluril molecules (cf. Figure 2). The **1.2$_4$.1b** structure is more stable than the **1.2$_4$.1a** isomer by 0.1(0.4) eV at the M06-2X(PBE0 or ωB97X-D)/6-31G(d,p) level of theory (see Figure 2 and Table 2S of the SI). The encapsulation of *trans*-stilbene in the **1.2$_4$.1a** and **1.2$_4$.1b** cages also results in two minima, **1.2$_4$.1a_t** and **1.2$_4$.1b_t**, with the second found to be the most stable by about 0.2 eV (see Figure 3 and Table 2S of the SI). It might be noted that the experimental work refers to the **1.2$_4$.1a_t** complex.[29]

The geometries of the calculated free and encapsulated structures are given in Table 1 (B3LYP, PBE0, and M06-2X) and in Table 5S of the SI (all five different functionals). In general, similar geometries are obtained by employing the different functionals (cf. Tables 1 and 5S). In the free and encapsulated *trans*-stilbene, the dihedral angle of twist ($C_4C_2C_1C_3$) is calculated to be very close to 180° in all cases (see Table 1 and Table 5S of the SI). In general the results show that the geometry of encapsulated *trans*-stilbene in the **1.2$_4$.1** cage (**a** or **b** isomer) is nearly the same as that of free *trans*-stilbene, with only some small differences in the dihedral

dx.doi.org/10.1021/ja211164b | J. Am. Chem. Soc. 2012, 134, 4346−4354

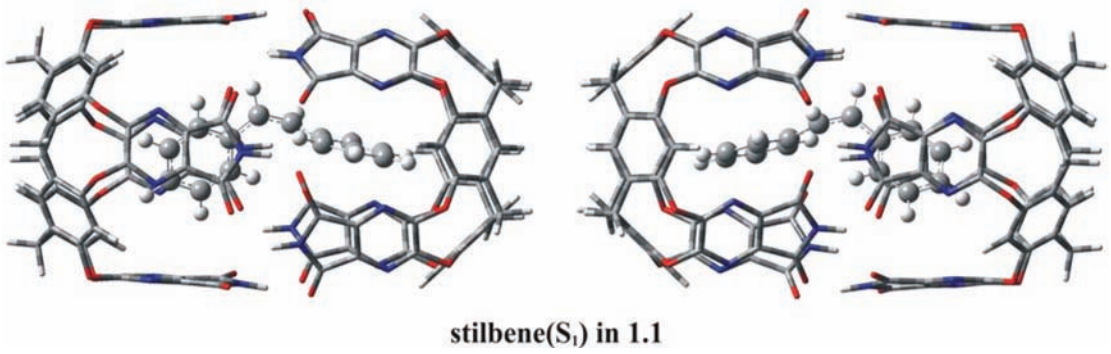

Figure 4. Minimum energy structure of stilbene in the **1.1** cage, in the first excited state of stilbene viewed from two different angles. This structure corresponds to the S_1 global minimum at the conical intersection.

Table 2. BSSE Corrected Interaction Energies, ΔE^a (eV), Using Different Functionals in Conjunction with the 6-31G(d,p) Basis Set

	1.1a	**1.1b**	**1.2$_4$.1a**	**1.2$_4$.1b**	**1.1a_t**		**1.1b_t**		**1.2$_4$.1a_t**		**1.2$_4$.1b_t**	
method	ΔE_1	ΔE_1	ΔE_1	ΔE_1	ΔE_2	ΔE_3	ΔE_2	ΔE_3	ΔE_2	ΔE_3	ΔE_2	ΔE_3
B3LYP	2.03[b]	2.08	6.48	6.71	−0.21[b]	1.84[b]	−0.20	1.88	−0.45	5.99	−0.48	6.21
PBE0	2.29	*d*	6.60	7.19	*d*	*d*	0.11	2.48	0.24	6.91	0.02	7.18
M06-2X	3.01	*d*	7.21	7.45	*d*	*d*	1.01	4.04	0.97	8.10	1.02	8.28
ωB97X-D[c]	2.90	*d*	7.95	8.45	*d*	*d*	1.83	4.74	1.58	9.45	1.63	10.02

[a] ΔE_1, energy of formation of the capsules; ΔE_2, energy of formation of the encapsulation complexes with respect to free stilbene and the capsules; ΔE_3, energy of formation of the encapsulation complexes with respect to free stilbene and the capsule constituents. [b] The CAM-B3LYP values are ΔE_1 = 2.51 eV for the **1.1a** and ΔE_2 = 0.08, ΔE_3 = 2.60 eV for the **1.1a_t**. [c] ωB97X-D/6-31G(d,p)//M06-2X/6-31G(d,p). [d] No stable structure obtained.

angle between the two phenyl groups, which is 0.4(0.5)° in free *trans*-stilbene, 3.4(16.5)° in the encapsulated one in the **1.2$_4$.1a** cage, and 0(0)° in the encapsulated one in the **1.2$_4$.1b** cage at the M06-2X(PBE0)/6-31G(d,p) levels of theory. As mentioned in the Introduction, the two phenyl groups in free *trans*-stilbene can rotate with a very low energy cost, and it is still a subject of controversy whether the optimum structure is planar.

In the case of encapsulated *trans*-stilbene in the **1.1** cage, there is a significant difference with the optimized geometry of free *trans*-stilbene: the dihedral angle between the two phenyl groups is calculated to be about 45°; i.e., it ranges between 41 to 49° with respect to different functionals (cf. Table 1). This can be seen in the structures of Figure 3, and in particular the end-on views, where the important difference between the larger and smaller cage encapsulation of *trans*-stilbene is illustrated. Conversely, when *cis*-stilbene is encapsulated in the small cage, i.e., **1.1**, it has the same geometry as free *cis*-stilbene (see Table 1).

The optimized geometries of the S_1 state of free and encapsulated *trans*-stilbene are also given in Table 1. As shown, the geometry of encapsulated *trans*-stilbene in the large cage, i.e., **1.2$_4$.1a** or **b**, at its first singlet excited state, S_1, is calculated to be the same as in the S_1 state of free *trans*-stilbene, and it corresponds to the local minimum at the trans geometry (see Scheme 1), which is calculated here to lie about 0.6 eV above the minimum at the conical intersection. In contrast, geometry optimization of the first excited singlet electronic state of the **1.1_t** encapsulation complex does not result in the local minimum of the excited free *trans*-stilbene but in the global minimum which is at the conical intersection with the ground state (see Figure 4 and Scheme 1). The angle of twist in the excited-state geometry is about 95°, and the dihedral angle between the phenyl groups is about 69° (cf. Table 1). This was

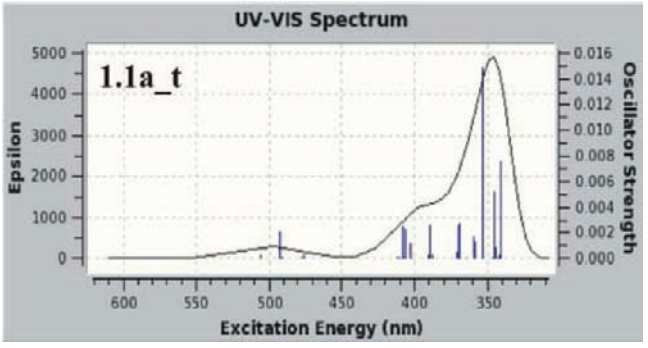

Figure 5. Absorption spectrum of the **1.1a_t** complex (first 60 roots) at the B3LYP/4-31G(d,p) level of theory.

obtained with all functionals employed. The reason for this is that in the case of the small cage the starting geometry for absorption corresponds to a different location at the excited-state surface from that of free *trans*-stilbene as the starting point of the geometry optimization. In this manner, the excited state of encapsulated stilbene in **1.1_t** does not emit, but it can decay nonradiatively through the conical intersection to the ground state, thus explaining the observed fluorescence quenching of *trans*-stilbene encapsulated in the small cage.[29]

Finally, it might be noted that the optimized geometry of the encapsulated stilbene via the ONIOM method, which is computationally faster by a factor of about 30, is nearly the same with the full DFT calculation (see Table 5S of the SI).

3.2. Energetics. The interaction energies (ΔE) of the calculated isomers are given in Table 2. As shown, use of the different functionals results in significant differences in some cases, with the PBE0, CAM-B3LYP, and B3LYP functionals leading to generally smaller interaction energies. The M06-2X

dx.doi.org/10.1021/ja211164b | J. Am. Chem. Soc. 2012, 134, 4346−4354

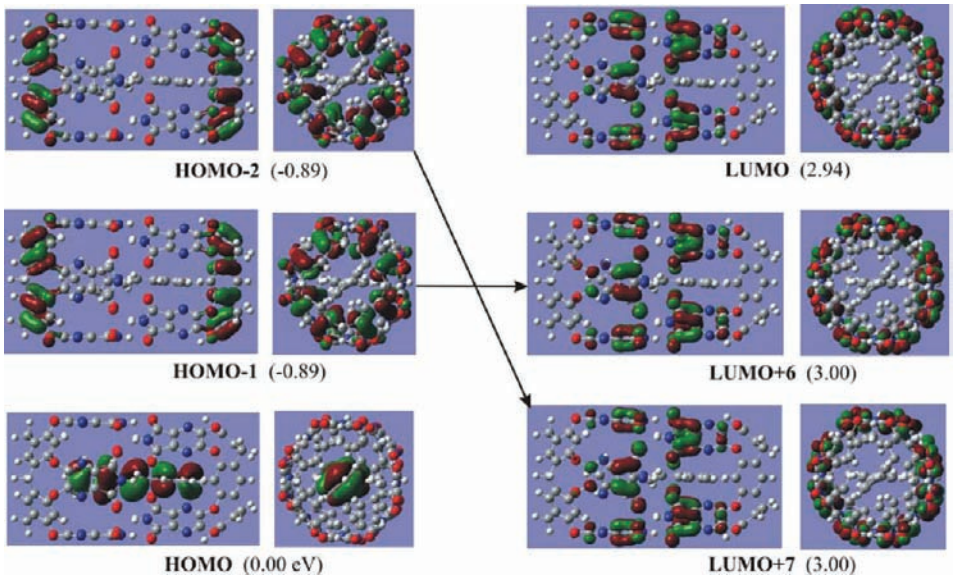

Figure 6. Electron density plots of the HOMO and LUMO molecular orbitals and of MO involved in the major peak at 353 nm of the absorption spectrum of the **1.1_t** species viewed from two different angles. The relative energies of the MO are given in parentheses.

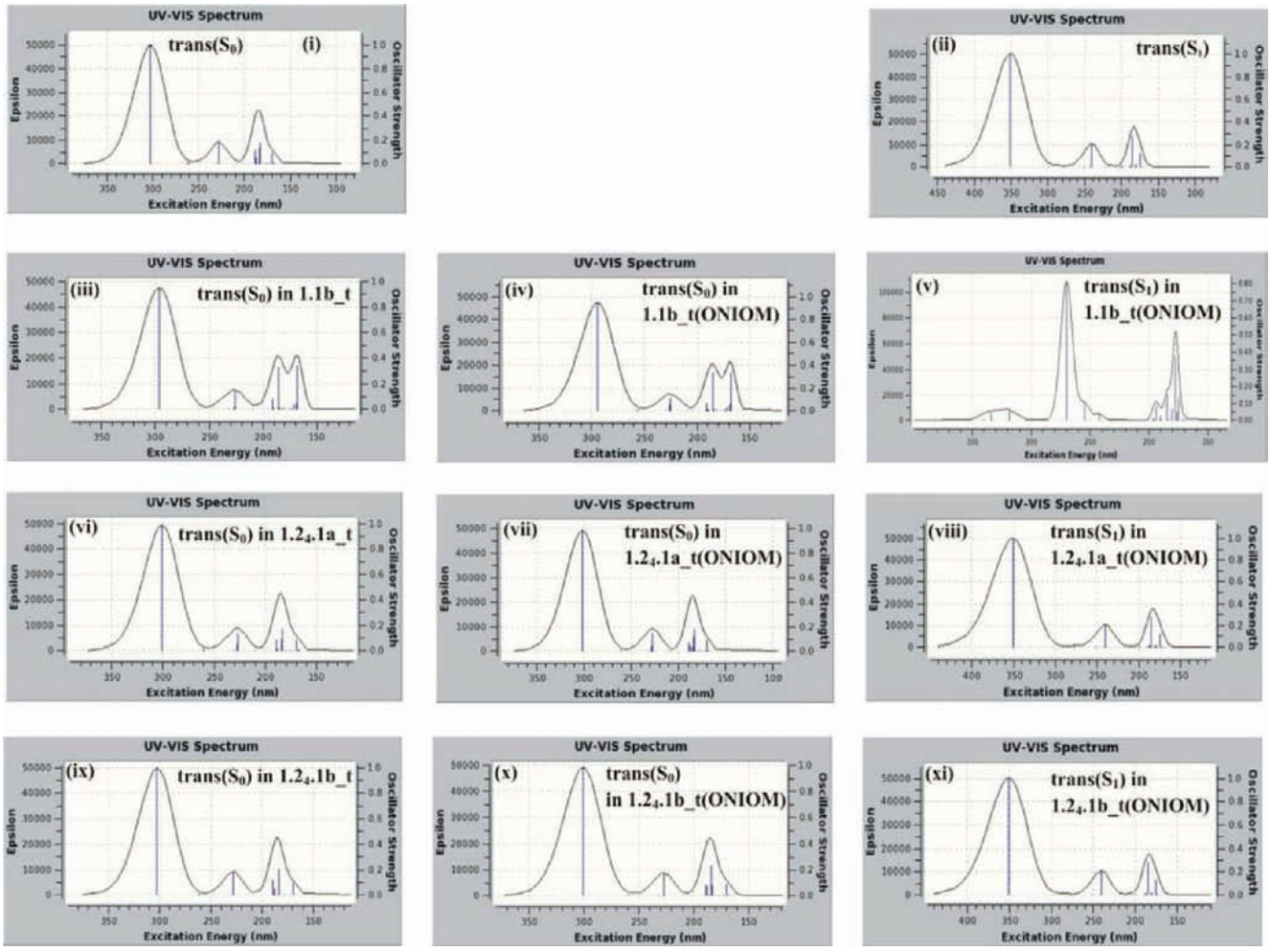

Figure 7. Absorption (under S_0) and emission (under S_1) spectra of the free and encapsulated *trans*-stilbene calculated at the PBE0/6-31G(d,p) and ONIOM(PBE0/6-31G(d,p):PM6) levels of theory.

and ωB97X-D functionals are considered to be more appropriate for bond energies, and accordingly greater confidence is placed in the corresponding data of Table 2. The ΔE_1 values refer to the formation energy of the cages **1.1a**, **1.2$_4$.1a**, and **1.2$_4$.1b** with respect to the two **1** cavitands (for **1.1a**) and with respect to the two **1** cavitands and four **2** spacers

dx.doi.org/10.1021/ja211164b | *J. Am. Chem. Soc.* 2012, 134, 4346−4354

Table 3. Vertical Excitation Energies, ΔE (eV), λ_{max} (nm), and *f*-Values for $S_0 \rightarrow S_1$ Absorption and $S_1 \rightarrow S_0$ Emission Maxima of Free and Encapsulated Stilbene at Various Levels of Theory in Conjunction with the 6-31G(d,p) Basis Set

				$S_0 \rightarrow S_1$					
	free *trans*-stilbene (S_0)			free *cis*-stilbene (S_0)			*trans*-stilbene (S_0) in **1.1b_t**[d]		
method	ΔE	λ_{max}	*f*-value	ΔE	λ_{max}	*f*-value	ΔE	λ_{max}	*f*-value
B3LYP	4.00	309.67	0.983	4.11	301.71	0.407	4.09	303.02	0.938
CAM-B3LYP	4.37	283.41	0.988	4.65	266.89	0.432	4.52	274.54	0.941
PBE0	4.10	302.52	0.998	4.23	292.82	0.396	4.19	296.12	0.955
M06-2X	4.39	282.48	0.997	4.66	265.92	0.385	4.51	274.99	0.935
ωB97X-D	4.53	273.60	0.951	4.69	264.58	0.407	4.51[f]	275.05[f]	0.928[f]
expt[a]	3.98[a], 4.22[a]			4.48[c]					
expt[b]	~4.0[b]								
	trans-stilbene (S_0) in **1.1b_t**[e]			*trans*-stilbene (S_0) in **1.2$_4$.1a_t**[d]			*trans*-stilbene (S_0) in **1.2$_4$.1b_t**[d]		
method	ΔE	λ_{max}	*f*-value	ΔE	λ_{max}	*f*-value	ΔE	λ_{max}	*f*-value
B3LYP	4.11	302.00	0.935	4.02	308.17	0.977	4.01	309.47	0.981
PBE0	4.21	294.43	0.950	4.12	300.90	0.989	4.10	302.49	0.996
M06-2X	4.53	273.45	0.952	4.41	281.01	0.978	4.38	283.37	0.983
ωB97X-D	4.51	274.68	0.955	4.41[f]	281.33[f]	0.969[f]	4.37[f]	283.78[f]	0.974[f]
	trans-stilbene (S_0) in **1.2$_4$.1a_t**[e]			*trans*-stilbene (S_0) in **1.2$_4$.1b_t**[e]			*cis*-stilbene (S_0) in**1.1a_t**[d]		
method	ΔE	λ_{max}	*f*-value	ΔE	λ_{max}	*f*-value	ΔE	λ_{max}	*f*-value
B3LYP	4.01	309.10	0.976	4.02	308.41	0.973	4.07	304.41	0.464
PBE	4.11	301.66	0.989	4.12	300.66	0.985			
				$S_1 \rightarrow S_0$					
	free *trans*-stilbene (S_1)			*trans*-stilbene (S_1) in **1.2$_4$.1a_t**[e]			*trans*-stilbene (S_1) in **1.2$_4$.1b_t**[e]		
method	ΔE	λ_{max}	*f*-value	ΔE	λ_{max}	*f*-value	ΔE	λ_{max}	*f*-value
B3LYP	3.47	357.40	0.999	3.47	357.77	0.996	3.47	357.67	0.996
CAM-B3LYP	3.62	342.69	0.991	3.61	343.11	0.988	3.62	342.91	0.988
PBE0	3.54	350.73	1.008	3.53	351.12	1.005	3.53	350.95	1.005
M06-2X	3.64	340.52	0.993	3.63	341.36	0.986	3.64	340.83	0.989
expt		363(361)[g]			358[h]				

[a]Reference 9a. [b]Reference 9e. [c]Reference 18b. [d]Stilbene in its optimized geometry inside the cage at the A/6-31G(d,p) level of theory, A = B3LYP, CAM-B3LYP, M06-2X, PBE0, ωB97X-D. [e]ONIOM(A/6-31 g(d,p):PM6), A = B3LYP, CAM-B3LYP, M06-2X, PBE0. [f]Stilbene in its optimized geometry inside the cage at the ωB97X-D/6-31G(d,p)//M06-2X/6-31G(d,p) level of theory. [g]Reference 29, 4,4′-diethylstilbene (4,4′-dimethylstilbene) in mesitylene. [h]Reference 29, 4,4′-diethylstilbene.

(for **1.2$_4$.1a** and **1.2$_4$.1b**). As shown, the cages are found to be stable with calculated ΔE_1 values of 3.01, 7.21, and 7.45 eV, respectively, at the M06-2X/6-31G(d,p) level of theory (see Table 2). The formation energies of the encapsulation complexes **1.1b_t**, **1.2$_4$.1a_t**, and **1.2$_4$.1b_t**, with respect to free *trans*-stilbene and cages **1.1** and **1.2$_4$.1**, given by the ΔE_2 values in Table 2, are calculated as 1.01(1.83), 0.97(1.58), and 1.02(1.63) eV at the M06-2X(ωB97X-D) levels of theory, while B3LYP results in −0.21 eV, after the BSSE correction has been carried out. It might be noted that similar binding (ΔE_2) is obtained for *trans*-stilbene in the small cage as in the large cage. Significant stability of the above encapsulation complexes is calculated with respect to free stilbene and dissociated cages given by the ΔE_3 values in Table 2.

Finally, the encapsulation of *cis*-stilbene, calculated for comparison, resulted in the **1.1a_c** complex (cf. Figure 3), which presents ΔE_2 and ΔE_3 values smaller by 0.34 eV than for the encapsulation of *trans*-stilbene (**1.1a_t**) using the B3LYP functional.

3.3. Absorption and Emission Spectra. The absorption spectrum involving transitions to 60 singlet-spin excited electronic states of the encapsulated complex **1.1**_*trans*-stilbene is given in Figure 5, obtained by B3LYP/4-31G due to technical difficulties when attempting to use B3LYP/6-31G(d,p) on this complex. Test calculations on the spectrum of free *trans*-stilbene show only slight differences between the B3LYP/4-31G and the B3LYP/6-31G(d,p) results (see Figure 2S and Table 3S of the SI). Thus, we can conclude that the use of the B3LYP/4-31G basis set is adequate for this system. All 60 singlet-spin excited electronic states correspond to excitations to unoccupied orbitals of the cage. The oscillator strength of all peaks is very small; the major peak, calculated at 353 nm corresponds to the 39th excited state with oscillator strength of only 0.015. This excited state is characterized mainly by the excitations HOMO-2 →LUMO+7 and HOMO-1→ LUMO+6. The electron density plots of these frontier molecular orbitals along with the HOMO and LUMO orbitals are depicted in Figure 6. The HOMO orbital of the **1.1_t** complex is the HOMO orbital of stilbene. Excitations from this HOMO orbital to unoccupied orbitals of the cage have vanishing oscillator strengths. The energies of the first 60 singlet-spin excited electronic states of the encapsulated complex are very closely spaced; as shown in Figure 5, they cover the range between 506 and 340 nm, while the first peak of free stilbene at the same level of theory, i.e., B3LYP/4-31G, is at 301 nm. For this reason the ONIOM method is required for the calculation of the absorption spectra of encapsulated stilbene, while it is practically the only alternative for calculation of emission spectra, for which geometry relaxation at the excited state of encapsulated stilbene is required.

Absorption and emission spectra of free and encapsulated *trans*-stilbene calculated at different levels of theory are depicted

dx.doi.org/10.1021/ja211164b | J. Am. Chem. Soc. 2012, 134, 4346−4354

in Figure 7 and Figures 2S−6S of the SI. Vertical excitation energies $S_0 \rightarrow S_1$, λ_{max} corresponding to the major peaks, and oscillator strengths (*f*-values) of stilbene free or encapsulated in the **1.1** and **1.2$_4$.1** cages at various levels of theory are given in Table 3 and Tables 3S and 4S of the SI. In all cases, the main excitation is a HOMO→LUMO transition (see Tables 3S and 4S of the SI). Generally good agreement is obtained with available experimental transition energies, with the B3LYP and the PBE0 values being in the best agreement with experiment (cf. Table 3).

The absorption spectra of stilbene obtained by full TDDFT at its cage-optimized geometry and by the ONIOM technique are practically the same (cf. Table 3 and spectra (iii) and (iv), (vi) and (vii), (ix) and (x) in Figure 7 and also Figures 2S−6S of the SI). As we have already mentioned, the geometry of *trans*-stilbene inside the **1.2$_4$.1** cage is almost unaffected by the presence of the cage, and as a result the absorption spectra of free *trans*-stilbene and of the encapsulated one are similar (cf. spectra (i)−(vi) and (ix) in Figure 7 and Figures 2S−6S of the SI). The geometry of *trans*-stilbene inside the **1.1** cage has the two phenyl groups twisted, as discussed in the previous section, but there is no big effect on the absorption spectra, with only a small blue shift in the λ_{max} by 8 nm with respect to the spectrum of free *trans*-stilbene (see Table 3). Finally, the geometry of *cis*-stilbene does not change significantly inside the **1.1** cage, and as a result, the absorption spectra of free *cis*-stilbene and the encapsulated one are similar (see Figure 2S).

The emission spectra of free *trans*-stilbene and of the encapsulated *trans*-stilbene using the different functionals are depicted in Figure 7 (spectra (ii), (v), (viii), and (xi)) and Figures 2S−6S of the SI, while data for the $S_1 \rightarrow S_0$ excitation are also included in Table 3. We observe that for the **1.2$_4$.1** cage, the emission spectrum of stilbene is not affected by the presence of the cage (cf. spectra (ii), (viii), and (xi) in Figure 7), as was the case for the absorption spectrum above. This results from the fact that the optimized geometry of the excited (S_1) *trans*-stilbene is found to be nearly the same in the **1.2$_4$.1_t** complex as in free *trans*-stilbene. Thus, encapsulated *trans*-stilbene in **1.2$_4$.1** absorbs, then it relaxes to the geometry of free trans-excited stilbene, and finally it emits. This is in agreement with the experimental observation reported by Ams et al.,[29] where the fluorescence of the *trans*-stilbene in the **1.2$_4$.1** capsule is retained.

The calculated emission spectrum of *trans*-stilbene in the **1.1_t** complex shows no significant intensity in the wavelength region >300 nm (cf. Figure 7(v)). This is because the excited-state optimized geometry is at the conical intersection of S_1 and S_0 in this case, whereas in free *trans*-stilbene and also in the **1.2$_4$.1_t** complex the optimized geometry lies at the local minimum of S_1 at about 3.5 eV above S_0. Thus, encapsulated *trans*-stilbene, **1.1_t**, after the absorption to S_1 relaxes to the geometry of the global minimum and decays nonradiatively via the conical intersection to S_0. This explains why Ams et al.[29] found experimentally that stilbene fluorescence is quenched in the **1.1** capsule; i.e., the distortion of stilbene's ground-state geometry in the small cage affects the geometry of the excited state and leads to quenching of the fluorescence.

4. CONCLUSIONS

The encapsulation of *trans*-stilbene in the **1.1** and **1.2$_4$.1** capsules was studied using DFT and TDDFT methodology at the B3LYP, CAM-B3LYP, M06-2X, PBE0, and ωB97X-D/6-31G(d,p) levels of theory. Absorption and emission spectra of free and encapsulated stilbene were calculated. For the emission spectra of encapsulated stilbene, the ONIOM method was required in order to carry out optimization of the excited-state geometry of stilbene within the cage. The main objective of the present study was the interpretation of the experimental observation of quenching of fluorescence of stilbene in the smaller **1.1** capsule but not in the **1.2$_4$.1** capsule.[29]

The results show that the ground-state geometry of encapsulated stilbene in the large cage, **1.2$_4$.1**, is nearly the same as that of free *trans*-stilbene. Similarly, the geometry determined for the excited state of *trans*-stilbene in the **1.2$_4$.1_t** encapsulation complex is the same as that of the excited state of free *trans*-stilbene at a local minimum of the excited-state surface. As a result, the absorption and emission spectra of *trans*-stilbene are not affected by encapsulation in the **1.2$_4$.1** cage.

In contrast, encapsulation of *trans*-stilbene in the **1.1** cage results in significant modification of the ground-state geometry, involving twisting of the two phenyl groups. The effect on the calculated absorption spectra is a small blue shift by 8 nm in λ_{max}. However, a major effect is found on the emission spectrum of the encapsulated stilbene as compared to that of free *trans*-stilbene: The present study shows that the distortion of *trans*-stilbene's ground-state geometry causes the geometry optimization at the excited state to converge to the global minimum of the S_1 state at the conical intersection. As a result, there is no emission similar to that of free *trans*-stilbene, and the state decays nonradiatively to the ground state.

The present work provides an interpretation of the experimental observation that stilbene fluorescence quenches in the **1.1** capsule, while in the **1.2$_4$.1** capsule the fluorescence returns.[29] In this manner, the unexpected results on stilbene fluorescence in the constrained environment in view of the antibody studies[30] have been explained.

■ ASSOCIATED CONTENT

Ⓢ Supporting Information

Tables 1S−4S, absolute and relative energies, vertical excitation energies, absorption or emission major peaks, oscillator strengths, main excitations coefficient contributing to the excited state of the calculated structures at various levels of theory; Tables 5S and 6S, geometry and Cartesian coordinates of the calculated species at various levels of theory; Figures 1S, structures of the calculated species viewed from different angles; Figures 2S−6S, absorption and emission spectra of the free and encapsulated *trans*- and *cis*-stilbene calculated at various levels of theory; additional references on photo-isomerization of stilbene. This material is available free of charge via the Internet at http://pubs.acs.org.

■ AUTHOR INFORMATION

Corresponding Author

idpet@eie.gr

Notes

The authors declare no competing financial interest.

■ ACKNOWLEDGMENTS

Financial support from the NATO grant CBP.MD.CLG.983711 is gratefully acknowledged.

■ REFERENCES

(1) Waldeck, D. H. *Chem. Rev.* **1991**, *91*, 415.
(2) Meier, H. *Angew. Chem.* **1992**, *31*, 1399.
(3) Arai, T.; Tokumaru, K. *Chem. Rev.* **1993**, *93*, 23.

(4) Whitten, D. G. *Acc. Chem. Res.* **1993**, *26*, 502.
(5) Görner, H.; Kuhn, H. J. *Adv. Photochem.* **1995**, *19*, 1.
(6) Fuss, W.; Kosmidis, C.; Schmid, W. E.; Trushin, S. A. *Angew. Chem., Int. Ed.* **2004**, *43*, 4178.
(7) Scholes, G. D.; Larsen, D. S.; Fleming, G. R.; Rumbles, G.; Burn, P. L. *Phys. Rev. B* **2000**, *61*, 13670.
(8) Hide, F.; Diaz-Garcia, M. A.; Schwartz, B. J.; Andersson, M. R.; Pei, Q.; Heeger, A. J. *Science* **1996**, *273*, 1833.
(9) See, for instance: (a) Suzuki, H. *Bull. Chem. Soc. Jpn.* **1960**, *33*, 379. (b) Bernstein, J. *Spectrochim. Acta* **1973**, *29A*, 147. (c) Traetteberg, M.; Frantsen, E. B.; Mijlhoff, F. C.; Hoekstra, A. *J. Mol. Struct.* **1975**, *26*, 57. (d) Fuke, K.; Sakamoto, S.; Ueda, M.; Itoh, M. *Chem. Phys. Lett.* **1980**, *74*, 546. (e) Hohlneicher, G.; Dick, B. *J. Photochem.* **1984**, *27*, 215. (f) Ni, T.; Caldwell, R. A.; Melton, L. A. *J. Am. Chem. Soc.* **1989**, *111*, 457. (g) Ikeyama, T.; Azumi, T. *J. Phys. Chem.* **1994**, *98*, 2832. (h) Ogawa, K.; Harada, J.; Tomoda, S. *Acta Crystallogr.* **1995**, *B51*, 240.
(10) Petek, H.; Yoshihara, K.; Fujiwara, Y.; Lin, Z.; Penn, J. H.; Frederick, J. H. *J. Phys. Chem.* **1990**, *94*, 7539. Saltiel, J.; Waller, A. S.; Sears, D. F. Jr. *J. Am. Chem. Soc.* **1993**, *115*, 2453. Hohlneicher, G.; Wrzal, R.; Lenoir, D.; Frank, R. *J. Phys. Chem. A* **1999**, *103*, 8969. Oelgemoller, M.; Brem, B.; Frank, R.; Schneider, S.; Lenoir, D.; Hertkorn, N.; Origane, Y.; Lemmen, P.; Lex, J.; Inoue, Y. *J. Chem. Soc., Perkin Trans. 2* **2002**, 1760.
(11) Syage, J. A.; Felker, P. M.; Zewail, A. H. *J. Chem. Phys.* **1984**, *81*, 4685. Syage, J. A.; Felker, P. M.; Zewail, A. H. *J. Chem. Phys.* **1984**, *81*, 4706. Baskin, J. S.; Banares, L.; Pedersen, S.; Zewail, A. H. *J. Phys. Chem.* **1996**, *100*, 11920.
(12) Takeuchi, S.; Ruhman, S.; Tsuneda, T.; Chiba, M.; Taketsugu, T.; Tahara, T. *Science* **2008**, *322*, 1073. Sajadi, M.; Dobryakov, A. L.; Garbin, E.; Ernsting, N. P.; Kovalenko, S. A. *Chem. Phys. Lett.* **2010**, *489*, 44.
(13) Bao, J.; Weber, P. *J. Phys. Chem. Lett.* **2010**, *1*, 224.
(14) Dietl, C.; Papastathopoulos, E.; Nicklaus, P.; Improta, R.; Santoro, F.; Gerber, G. *Chem. Phys.* **2005**, *310*, 201.
(15) Frederick, J. H.; Fujiwara, Y.; Penn, J. H.; Yoshihara, K.; Petek, H. *J. Phys. Chem.* **1991**, *95*, 2845. Langkilde, F. W.; Wilbrandt, R.; Brouwer, A. M.; Negri, F.; Zerbetto, F.; Orlandi, G. *J. Phys. Chem.* **1994**, *98*, 2254.
(16) (a) Watanabe, H.; Okamoto, Y.; Furuya, K.; Sakamoto, A.; Tasumi, M. *J. Phys. Chem.* **2002**, *106*, 3318. (b) Sakamoto, A.; Tanaka, F.; Tasumi, M.; Torii, H.; Kawato, K.; Furuya, K. *Vibration Spectrosc.* **2006**, *42*, 176.
(17) Beveridge, D. L.; Jaffé, H. H. *J. Am. Chem. Soc.* **1965**, *87*, 5340. Todd, D. C.; Fleming, G. R.; Jean, J. M. *J. Chem. Phys.* **1992**, *97*, 8915.
(18) (a) Molina, V.; Merchán, M.; Roos, B. O. *J. Phys. Chem. A* **1997**, *101*, 3478. (b) Molina, V.; Merchàn, M.; Roos, B. O. *Spectrochim. Acta, Part A* **1999**, *55*, 433. (c) Gagliardi, L.; Orlandi, G.; Molina, V.; Malmqvist, P.-A.; Roos, B. *J. Phys. Chem. A* **2002**, *106*, 7355. (d) Quenneville, J.; Martínez, T. J. *J. Phys. Chem. A* **2003**, *107*, 829.
(19) Orlandi, G.; Gagliardi, L.; Melandri, S.; Caminati, W. *J. Mol. Struct.* **2002**, *612*, 383. Freile, M. L.; Risso, S.; Curaqueo, A.; Zamore, M. A.; Enriz, R. D. *J. Mol. Struct. (Theochem)* **2005**, *731*, 107.
(20) Amatatsu, Y. *Chem. Phys. Lett.* **1999**, *314*, 364.
(21) Tatchen, J.; Pollak, E. *J. Chem. Phys.* **2008**, *128*, 164303.
(22) Chowdary, P. D.; Martínez, T. J.; Gruebele, M. *Chem. Phys. Lett.* **2007**, *440*, 7.
(23) Kwasniewski, S. P.; Claes, L.; François, J.-P.; Deleuze, M. S. *J. Chem. Phys.* **2003**, *118*, 7823.
(24) Improta, R.; Santoro, F.; Dietl, C.; Papastathopoulos, E.; Gerber, G. *Chem. Phys. Lett.* **2004**, *387*, 509. Improta, R.; Santoro, F. *J. Phys. Chem. A* **2005**, *109*, 10058.
(25) Bearpark, M. J.; Bernardi, F.; Clifford, S.; Olivucci, M.; Robb, M. A.; Vreven, T. *J. Phys. Chem. A* **1997**, *101*, 3841.
(26) Tsumura, K.; Furuya, K.; Sakamoto, A.; Tasumi, M. *J. Raman Spectrosc.* **2008**, *39*, 1584.
(27) Minezawa, N.; Gordon, M. S. *J. Phys. Chem. A* **2011**, *115*, 7901.
(28) Dou, Y.; Allen, R. E. *J. Chem. Phys.* **2003**, *119*, 10658.
(29) Ams, M. R.; Ajami, D.; Craig, S. L.; Yang, J.-S.; Rebek, J. Jr. *Beilstein J. Org. Chem.* **2009**, *5*, 79.
(30) Simeonov, A.; et al. *Science* **2000**, *290*, 307. Matsushita, M.; Meijler, M. M.; Wirsching, P.; Lerner, R. A.; Janda, K. D. *Org. Lett.* **2005**, *7*, 4943. Armitage, B. A.; Berget, P. B. *Science* **2008**, *319*, 1195. Debler, E. W.; et al. *Science* **2008**, *319*, 1232.
(31) Ajami, D.; Dube, H.; Rebek, J. Jr. *J. Am. Chem. Soc.* **2011**, *133*, 9689.
(32) Tzeli, D.; Theodorakopoulos, G.; Petsalakis, I. D.; Ajami, D.; Rebek, J. Jr *J. Am. Chem. Soc.* **2011**, *133*, 16977.
(33) Parthasarathy, A.; Kaanumalle, L. S.; Ramamurthy, V. *Org. Lett.* **2007**, *9*, 5059.
(34) Natarajan, A.; Kaanumalle, L. S.; Jockusch, S.; Gibb, C. L. D.; Gibb, B. C.; Turro, M. J.; Ramamurthy, V. *J. Am. Chem. Soc.* **2007**, *129*, 4132.
(35) Ams, M. R.; Ajami, D.; Craig, S. L.; Yang, J.-S.; Rebek, J. Jr. *J. Am. Chem. Soc.* **2009**, *131*, 13190.
(36) Dube, H.; Ajami, D.; Rebek, J. Jr. *Angew. Chem., Int. Ed.* **2010**, *49*, 3192.
(37) Ajami, D.; Rebek, J. Jr. *J. Org. Chem.* **2009**, *74*, 6584.
(38) Becke, D. *J. Chem. Phys.* **1993**, *98*, 1372. Lee, C.; Yang, W.; Parr, R. G. *Phys. Rev. B* **1988**, *37*, 785.
(39) (a) Yanai, T.; Tew, D.; Handy, N. *Chem. Phys. Lett.* **2004**, *393*, 51. (b) Peach, M. J. G.; Benfield, P.; Helgaker, T.; Tozer, D. J. *J. Chem. Phys.* **2008**, *128*, 044118. (c) Stein, T.; Kronik, L.; Baer, R. *J. Am. Chem. Soc.* **2009**, *131*, 2818.
(40) Zhao, Y.; Truhlar, D. G. *Theor. Chem. Acc.* **2008**, *120*, 215. Zhao, Y.; Truhlar, D. G. *Acc. Chem. Res.* **2008**, *41*, 157.
(41) (a) Perdew, J. P.; Burke, K.; Ernzerhof, M. *Phys. Rev. Lett.* **1996**, *77*, 3865. (b) Enzerhof, M.; Scuseria, G. E. *J. Chem. Phys.* **1999**, *110*, 5029. (c) Adamo, C.; Barone, V. *J. Chem. Phys.* **1999**, *110*, 6158.
(42) Chai, J.-D.; Head-Gordon, M. *Phys. Chem. Chem. Phys.* **2008**, *10*, 6615.
(43) Curtiss, L. A.; McGrath, M. P.; Blandeau, J.-P.; Davis, N. E.; Binning, R. C. Jr.; Radom, L. *J. Chem. Phys.* **1995**, *103*, 6104.
(44) Dapprich, S.; Komáromi, I.; Byun, K. S.; Morokuma, K.; Frisch, M. J. *J. Mol. Struct. (Theochem)* **1999**, *462*, 1. Vreven, T.; Morokuma, K.; Farkas, Ö.; Schlegel, H. B.; Frisch, M. J. *J. Comput. Chem.* **2003**, *24*, 760. Vreven, T.; Morokuma, K. *Annu. Rep. Comput. Chem.* **2006**, *2*, 35.
(45) Boys, S. F.; Bernardi, F. *Mol. Phys.* **1970**, *19*, 553.
(46) Tzeli, D.; Mavridis, A.; Xantheas, S. S. *J. Phys. Chem. A* **2002**, *106*, 11327.
(47) Marques, M. A. L.; Gross, E. K. U. *Annu. Rev. Phys. Chem.* **2004**, *55*, 427.
(48) Frisch, M. J.; et al. *Gaussian 09*, Revision A.1; Gaussian, Inc.: Wallingford, CT, 2009.